

F-segments of Arabidopsis dehydrins show cryoprotective activities for lactate dehydrogenase depending on the hydrophobic residues

メタデータ	言語: eng 出版者: 公開日: 2020-04-06 キーワード (Ja): キーワード (En): 作成者: Ohkubo, Tomohiro, Kameyama, Ayuko, Kamiya, Keita, Kondo, Mitsuru, Hara, Masakazu メールアドレス: 所属:
URL	http://hdl.handle.net/10297/00027252

1 **ORIGINAL PAPER**

2

3 **Title**

4 F-segments of *Arabidopsis* dehydrins show cryoprotective activities for lactate dehydrogenase
5 depending on the hydrophobic residues.

6

7 **Authors**

8 Tomohiro Ohkubo¹, Ayuko Kameyama¹, Keita Kamiya¹, Mitsuru Kondo^{1,2}, Masakazu Hara^{1*}

9

10 ¹Research Institute of Green Science and Technology,

11 Shizuoka University,

12 836 Ohya, Shizuoka, Shizuoka 422-8529, Japan

13

14 ²Department of Chemistry, Faculty of Science,

15 Shizuoka University,

16 836 Ohya, Shizuoka, Shizuoka 422-8529, Japan

17

18 ***Name and address for editorial correspondence**

19 Masakazu Hara

20 Research Institute of Green Science and Technology,

21 Shizuoka University,

22 836 Ohya, Shizuoka 422-8529, Japan

23 Tel: +81-54-238-5134

24 Fax: +81-54-238-5134

25 E-mail: hara.masakazu@shizuoka.ac.jp

26

27 **Abstract**

28 Although dehydrins show cryoprotective activities for freeze-sensitive enzymes, the underlying
29 mechanism is still under investigation. Here, we report that F-segments conserved in some dehydrins
30 cryoprotected lactate dehydrogenase (LDH) as well as K-segments, which were previously identified
31 as cryoprotective segments of dehydrins. The cryoprotective activity levels of four F-segments of

32 *Arabidopsis* dehydrins were similar to that of a typical K-segment. Amino acid substitution
33 experiments indicated that the activity of the F-segment of *Arabidopsis* COR47 (designated as Fseg)
34 depended on the hydrophobic residues (L, F, and V). Intriguingly, when all the amino acids other
35 than the hydrophobic residues were changed to glycine, the cryoprotective activity did not change,
36 suggesting that the hydrophobic amino acids were sufficient for Fseg activity. Circular dichroism
37 analysis indicated that Fseg was mainly disordered in aqueous solution as well as Fseg_Φ/T, in
38 which the hydrophobic residues of Fseg were changed to T. This suggested that the hydrophobic
39 interaction might be related to the cryoprotective activities of Fseg.

40

41

42 **Keywords** *Arabidopsis thaliana* (Brassicaceae); protein function; late embryogenesis abundant
43 (LEA) proteins; dehydrins

44

45

46 **1. Introduction**

47

48 When plants are exposed to stresses, a series of late embryogenesis abundant (LEA) proteins are
49 expressed (Hundertmark and Hinch, 2008; Hand et al., 2011). Expression of dehydrins, which are
50 group 2 LEA proteins, is a major response to abiotic stresses such as cold, drought, and high salinity
51 (Eriksson and Harryson, 2011; Graether and Boddington, 2014; Banerjee and Roychoudhury, 2016)
52 as well as to biotic stresses (Hanin et al., 2011). Because the amino acid sequences of dehydrins are
53 dissimilar to those of any previously identified proteins, functional studies of them are still under
54 way; nevertheless it has been believed that dehydrins may function as protectants for stressed plants
55 according to the results of transgenic studies (Banerjee and Roychoudhury, 2016). Dehydrins are
56 detected in various tissues and subcellular compartments, such as cytoplasm, nucleus, plastid,
57 mitochondrion, endoplasmic reticulum, and plasma membrane (reviews cited above). The ubiquitous
58 distribution of dehydrins indicates that they protect whole cells from damage caused by stresses.

59 Dehydrins are classified as intrinsically disordered proteins, since the proportion of hydrophilic
60 residues is far greater than that of hydrophobic residues in the sequences. The flexibility of
61 dehydrins has been observed with various analytical methods such as circular dichroism (CD),
62 Fourier-transform infrared spectroscopy (FTIR), and nuclear magnetic resonance (NMR) (Findlater
63 and Graether, 2009; Rahman et al., 2011; Ágoston et al., 2011; Clarke et al., 2015). Dehydrins have
64 conserved sequences, e.g., K-, Y-, and S-segments (Close, 1997). K-segments (e.g.,
65 EKKGIMEKIKEKLP) are essential for identifying dehydrins. Y-segments (e.g., DEYGNP) and

66 S-segments (e.g., LHRSGSSSSSSSEDD) are frequently found in some dehydrins. By using the
67 shorthand notation of K, Y, and S, dehydrins are conventionally classified as SKn, FSKn, KnS, Kn,
68 YnSKn, YnKn, etc. Besides them, Φ -segments, which are rich in G and polar amino acids (Close,
69 1997), PK (polylysine)-segments (Hara et al., 2009), and F-segments (DRGLFDLFGKK or extended
70 ones) (Strimbeck, 2017; Wei et al., 2019) have been proposed. Many studies have reported that such
71 segments had corresponding functions *in vitro*. K-segments showed cryoprotective activities for
72 freeze-sensitive enzymes such as lactate dehydrogenase (LDH, EC 1.1.1.27) (Hughes et al., 2013;
73 Hara et al., 2017). K-segments are also involved in the binding to negatively charged lipids (Koag et
74 al., 2009). The membrane binding of dehydrins might maintain the fluidity of membranes at low
75 temperature (Eriksson et al., 2011; Clarke et al. 2015). S-segments are likely Ca^{2+} binding sites of
76 dehydrins when the segments are phosphorylated (Alsheikh et al., 2003). The polar Φ -segments
77 might be involved in the great flexibility of dehydrins. The PK-segment and K-rich area of dehydrins
78 are related to the DNA binding (Hara et al., 2009; Boddington and Graether, 2019). Although
79 specific segments have not been identified, the H residues and H-rich regions were proposed to bind
80 to transition metals (Hara et al., 2005), reduce the generation of reactive oxygen species (Hara et al.,
81 2013), and regulate the lipid binding of dehydrins (Eriksson et al., 2011). However, the functions of
82 F-segments, which are well conserved in cold-responsive FSKn dehydrins, are still unknown.

83 Since cold is a general environmental cue for dehydrin expression in plants, the physiological
84 roles of dehydrins in cold-stressed plants have been intensively studied. Although diverse transgenic
85 experiments revealed that the high expression levels of dehydrin genes enhanced the cold tolerance
86 of plants (e.g., Hara et al., 2003; Puhakainen et al., 2004; Peng et al., 2008; Xing et al., 2011;
87 Ochoa-Alfaro et al., 2012; Zhang et al., 2018), how dehydrins act during the establishment of cold
88 tolerance *in planta* has not been confirmed but is now under investigation. Many studies have
89 investigated the cryoprotection of freeze-sensitive enzymes by dehydrins (e.g., Hara et al., 2001;
90 Bravo et al., 2003; Hughes and Graether, 2011; Drira et al., 2013). It was demonstrated that size is
91 one of the most important factors in the cryoprotective activities of dehydrins (Hughes et al. 2013).
92 In addition, truncation experiments indicated that K-segments of ERD10, RcDhn5, TaDHN-5, and
93 WZY2 were necessary to exhibit the full inhibitory activities of the dehydrins for the cold
94 denaturation of LDH (Reyes et al., 2008; Drira et al., 2013; Yang et al., 2015). As described above,
95 K-segments even alone inhibited freezing damage to LDH, suggesting that K-segments might be
96 related to the cryoprotective activities of dehydrins. However, no cryoprotective sites other than
97 K-segments have been determined in dehydrins.

98 Recently, it was reported that when the hydrophobic amino acids of a K-segment were changed to
99 polar uncharged Ts, the cryoprotective activity of the K-segment was remarkably reduced (Hara et
100 al., 2017). In this case, at least three hydrophobic residues were needed for the cryoprotective
101 activity. This supported the idea that the segments containing multiple hydrophobic residues might

102 show cryoprotective activities. From this point of view, we predicted that F-segments may have
103 cryoprotective activities like K-segments, because F-segments possessed hydrophobic core regions
104 (e.g., LFDL) in their sequences. Here we found that four F-segments of *Arabidopsis* FSKn
105 dehydrins showed potent cryoprotective activities for LDH and that the segment's hydrophobic
106 amino acids were necessary for the activities. The putative cryoprotective mechanisms of
107 F-segments were discussed on the basis of hydrophobic interaction.

108
109

110 **2. Results**

111

112 *2.1. Cryoprotective activities of F-segments*

113

114 F-segments are conserved in FSKn dehydrins. *Arabidopsis* possesses four FSKn dehydrin genes,
115 i.e., *At1g20440* (*COR47*, FSK3), *At1g20450* (*ERD10*, FSK3), *At1g76180* (*ERD14*, FSK2), and
116 *At4g38410* (FSK2), all of which are expressed by cold stress (Supplemental Fig. 1). There was one
117 F-segment per FSKn dehydrin (Strimbeck, 2017). Four F-segments, COR47Fseg, ERD10Fseg,
118 ERD14Fseg, and At4g38410Fseg, were tested (Fig. 1A). The sequence lengths were adjusted to 15
119 amino acids because we compared their cryoprotective activities to the positive standard: the typical
120 K-segment (TypK) possessing 15 amino acids (Hara et al., 2017).

121 To estimate the cryoprotective activities, we measured the inhibition of both cryoinactivation and
122 cryodenaturation for LDH (Fig. 1B, C). LDH has been widely used as a model enzyme for
123 cryoprotection studies because it is sensitive to low temperature. Cryoinactivation was determined
124 by the enzymatic activities of LDH before and after the freeze and thaw treatments (Supplemental
125 Fig. 2A, B). Cryodenaturation was analyzed by monitoring the hydrophobicity of LDH during the
126 freeze and thaw cycles by 8-anilino-1-naphthalene sulfonic acid (ANS), which is a detector of the
127 surface hydrophobicity of proteins (Supplemental Fig. 2C). The F-segment peptides effectively
128 inhibited the cryoinactivation and cryodenaturation of LDH by the same magnitude as TypK (Fig.
129 1B, C). The activity levels were similar to each other. This demonstrated that the F-segment peptides
130 had efficient cryoprotective activities for LDH. The following experiments were performed by using
131 COR47Fseg because its sequence was identical to that of the F-segment defined in the previous
132 report (Strimbeck, 2017). COR47Fseg is designated simply as Fseg in the text below.

133

134 *2.2. Role of hydrophobic residues*

135

136 We previously reported that the cryoprotective activity of TypK for LDH depended on the
137 hydrophobic residues in the TypK sequence (Hara et al., 2017). This implies that, also in the case of

138 Fseg, hydrophobic residues may be crucial for cryoprotective activity. To test this, we examined a
139 series of Fseg-altered peptides with various amino acid substitutions (Fig. 2). A hydrophobic
140 residues-to-T substitution peptide (Fseg_Φ/T), a negatively charged residues-to-T substitution
141 peptide (Fseg_DE/T), and a positively charged residues-to-T substitution peptide (Fseg_KR/T) were
142 prepared. The cryoprotective analyses indicated that Fseg_Φ/T totally lost its inhibition of LDH
143 cryoinactivation and cryodenaturation, but Fseg_DE/T and Fseg_KR/T still efficiently inhibited
144 cryoinactivation and cryodenaturation, to the same degree as Fseg. When hydrophobic residues were
145 changed to E (Fseg_Φ/E) and K (Fseg_Φ/K), their inhibition activities diminished. These results
146 suggested that the hydrophobic residues played an important role in the cryoprotective activity of
147 Fseg.

148 Since it was revealed that hydrophobic residues of Fseg were necessary for cryoprotective activity,
149 we changed the other amino acids to G (pG_Fseg_Φ) in order to clarify whether the hydrophobic
150 residues were sufficient for the activity (Fig. 3). Surprisingly, the pG_Fseg_Φ peptide showed
151 similar activity to Fseg in the inhibition of both LDH cryoinactivation and cryodenaturation. In
152 addition, the pG_Fseg_Φ-related peptides, which contained negatively charged residues
153 (pG_Fseg_ΦDE) or positively charged residues (pG_Fseg_ΦKR), also showed apparent activities.
154 On the other hand, altered peptides in which G was substituted for amino acids other than charged
155 residues (pG_Fseg_DE, pG_Fseg_KR, and pG_Fseg_DEKR) showed lower activity levels. The
156 present results demonstrated that the hydrophobic residues were necessary and sufficient to exhibit
157 the cryoprotective activity of Fseg.

158

159 *2.3. Structural features of Fseg*

160

161 In order to elucidate the mode of action underlying the cryoprotective activity of Fseg, we
162 compared the secondary structures between Fseg (the active peptide) and Fseg_Φ/T (the inactive
163 one) by using CD. We collected CD data on the solutions of Fseg and Fseg_Φ/T in 10 mM Tris
164 buffer pH 7.5 (Fig. 4A). Both peptides showed typical disordered states, which are expressed by
165 very negative values around 200 nm, whereas the sign of disorder in Fseg was weaker than that in
166 Fseg_Φ/T.

167 It has been documented that K-segments in solution showed a disorder-to-helix transition by the
168 addition of sodium dodecyl sulfate (SDS), and this transition may be related to the molecular
169 function of dehydrins (Koag et al., 2009). When we added SDS to the Fseg and Fseg_ΦT solutions,
170 little transition was observed except that the α -helix and β -strand in Fseg were increased slightly but
171 significantly by the addition of a high concentration of SDS (10 mM) (Fig. 4A, B). This suggested
172 that the cryoprotective activity of Fseg was not correlated with the capability of a structural
173 transition induced by SDS. Moreover, it is likely that Fseg did not interact with the membrane.

174 We obtained more information on the structural difference between Fseg and Fseg_ΦT by using
175 the de novo structure prediction system PEP-FOLD3 (Lamiable et al., 2016)
176 (<http://bioserv.rpbs.univ-paris-diderot.fr/services/PEP-FOLD3/>). Because this system was designed
177 for the structured peptides, we have to consider that the images represented one of the structures that
178 the peptides could have. The results showed that the 3D structures were clearly different between
179 Fseg and Fseg_ΦT. Fseg had a hydrophobic space in the middle of the structure (Supplemental Fig.
180 3A). The four hydrophobic amino acids (L₄, F₅, F₇, and L₈) each formed a hydrophobic area that was
181 exposed to the solvent. On the other hand, Fseg_ΦT did not have any hydrophobic area and the
182 whole structure was disordered for the most part (Supplemental Fig. 3B). We also built predictive
183 structures of other cryoprotective peptides used in this study, i.e., three F-segments (ERD10Fseg,
184 ERD14Fseg, and At4g38410Fseg), pG_Fseg_Φ, and TypK (Supplemental Fig. 3C), and found that
185 all of them possessed hydrophobic spaces as Fseg did. Intriguingly, their hydrophobic areas were
186 made by four hydrophobic amino acids and were exposed to the solvent, even though their amino
187 acid sequences were different.

188
189

190 **3. Discussion**

191

192 Although the cryoprotective activities of K-segments have been well documented, it has not been
193 investigated whether other segments also show such activities. Previous studies have reported that
194 FSKn-type dehydrin COR47 was related to the cold tolerance of *Arabidopsis*. The COR47 gene was
195 expressed and the protein was accumulated in the whole *Arabidopsis* plant with a specific response
196 to cold stress (Nylander et al., 2001). Overexpression of the COR47 gene enhanced the freezing
197 tolerance of *Arabidopsis* by coexpression with the RAB18 gene (Puhakainen et al., 2004).
198 OpsDHN1, a cold-responsive FSKn-type dehydrin of *Opuntia streptacantha* (Ochoa-Alfaro et al.,
199 2012), effectively protected LDH during the freeze and thaw process (Hernández-Sánchez et al.,
200 2014). Recently, FSKn-type-specific conserved segments, i.e., F-segments, have been identified
201 (Strimbeck, 2017; Wei et al., 2019). The sequence conservation of F-segments was higher than that
202 of K-segments in the COR47 orthologues from angiosperms (Supplemental Fig. 4), implying that
203 F-segments have been conserved during evolution, probably due to their important functions. Here
204 we report that the F-segments of four FSKn-type dehydrins showed the LDH cryoprotective activity
205 of the same potency as K-segments (Fig. 1).

206 A previous report demonstrated that the cryoprotective activity of a K-segment depended on the
207 hydrophobic residues of the peptide (Hara et al., 2017). Therefore, we tested whether the
208 hydrophobic residues of Fseg contributed to the cryoprotective activities. The experiments with
209 amino acid substitutions indicated that hydrophobic amino acids were the determining factors for the

210 cryoprotective activity of Fseg. Since the changes in positively charged amino acids to T somewhat
211 but significantly reduced cryoprotective activities (Fig. 2B, C), the positively charged amino acids
212 might be partially related to those activities.

213 It was confirmed that amino acid length is a major determinant of the cryoprotective activities of
214 dehydrins (Hughes et al. 2013). Moreover, the altered dehydrins, whose sequences were scrambled,
215 exhibited considerable activities (Palmer et al. 2019). On the other hand, K-segments alone showed
216 apparent cryoprotective activities and hydrophobic amino acids of K-segments were related to those
217 activities. Taken together these findings indicate that, although the size of the disordered region is
218 essentially important for cryoprotective activity, the amino acid sequences of segments may also be
219 responsible for the activities of dehydrins.

220 Here, the discussion moves to the mechanism underlying the LDH cryoprotective activities of
221 F-segments. In general, a molecular shield model (many reviews, e.g., Chakrabortee et al., 2012) has
222 been proposed to explain how dehydrins show cryoprotective activity (Hughes et al., 2013). The
223 aggregation of target proteins can be inhibited by the molecular shields of dehydrins with large
224 hydrodynamic radii due to the intrinsically disordered nature of those dehydrins. F-segments might
225 also function as molecular shields, because Fseg was in the disordered state determined by CD.
226 However, it is still unknown why hydrophobic amino acids were necessary for the cryoprotective
227 activity of Fseg. As shown in Supplemental Fig. 3, Fseg was postulated to have a hydrophobic area
228 that was exposed to the solvent. Similar hydrophobic areas were found in not only other F-segments
229 but also pG_Fseg_Φ and TypK, all of which showed cryoprotective activities, suggesting that such
230 hydrophobic areas might be crucial for cryoprotective peptides. In line with this idea, a scheme
231 describing the cryoprotective mechanism of Fseg is shown in Fig. 5. During the freeze and thaw
232 process, freeze-sensitive enzymes such as LDH lose their activities by aggregating together through
233 the hydrophobic patches on protein surfaces (Zhang et al., 2011) (Fig. 5A). The hydrophobic area of
234 Fseg might intervene in the hydrophobic interaction between target proteins. Since the hydrophobic
235 area of Fseg was not structurally complemented with the hydrophobic patches of proteins, the
236 interference by hydrophobic interaction could be transient. While Fseg inhibited aggregation,
237 hydrophobic hydration (Davis et al., 2012) might cover the patches of protein surfaces. Thus, LDH
238 is successfully kept active after the freeze and thaw process (Fig. 5B). It has been hypothesized that
239 group 4 LEA proteins and chaperones might interact with the target proteins (Cuevas-Velazquez et al.
240 2017; Tompa and Csermely, 2004), suggesting that the transient hydrophobic interactions might
241 function also in the case of the group 4 LEA proteins and the chaperones. On the other hand,
242 Fseg_Φ/T, which does not possess a hydrophobic area, cannot efficiently intervene in the
243 hydrophobic interaction between the proteins. As a result, Fseg_Φ/T might be excluded from the
244 hydrophobic space, after which the proteins would be aggregated due to the formation of water-tight
245 seals between the proteins (Fig. 5C).

246 Since the hydrophobic areas of F-segments consisted of L(M)FDFL, the sequences were certainly
247 thought to be the cores of the cryoprotective activities. It is noteworthy that the sequence of
248 L(M)FDFL was similar to the FXF motifs (e.g., the FNFL segment) related to the hydrophobic
249 interaction between mitogen-activated protein kinases and their partner proteins (Mace et al., 2013;
250 Liu et al., 2016). This implies that L(M)FDFL can affect the hydrophobic interactions between
251 proteins. Moreover, it is interesting that the configurations of hydrophobic areas were similar among
252 the cryoprotective peptides (Supplemental Fig. 3). In the case of F-segments, two Fs were positioned
253 like spreading arms and two Ls (or an L and an M) were located between the F arms. This formed
254 horizontally long hydrophobic areas. On the other hand, TypK was postulated to form a helix-like
255 structure. The four hydrophobic amino acids that were located on one side of the helix made a long
256 horizontal hydrophobic region, as did the F-segments. Moreover, exposure of the hydrophobic areas
257 to the solvent may enhance accessibility to hydrophobic patches on the surface of proteins. This may
258 facilitate the transient intervention for the hydrophobic interaction between proteins. It is suggested
259 that if the peptides were all the same size, the cryoprotective activities were determined mainly by
260 the configurations of the hydrophobic areas rather than by the primary and secondary structures of
261 the peptides.

262 In conclusion, we found that F-segments had cryoprotective activities as much as K-segments did.
263 This indicates that K-segments and F-segments may contribute to the cryoprotective activities of
264 cold-responsive FSKn-type dehydrins. Although dehydrins possess small amounts of hydrophobic
265 amino acids, the hydrophobic residues were key factors in the unique functions of dehydrins such as
266 protein cryoprotection. Further studies on the functions of dehydrins may provide useful information
267 on the physiological mechanisms underlying cold tolerance in plants and for the development of
268 high-performance cryoprotective agents.

269

270 **4. Experimental**

271

272 *4.1. Chemicals*

273

274 Rabbit muscle LDH (recombinant) and nicotine adenine dinucleotide (NADH) were purchased from
275 Oriental Yeast (Tokyo, Japan). ANS was obtained from Sigma (Tokyo, Japan). Peptides were
276 prepared by using an automated solid phase peptide synthesizer (Tetras, Advanced ChemTech,
277 Louisville, KY, USA). The peptides were purified by chromatography (UFLC-20AB, Shimadzu,
278 Kyoto, Japan) using a C18 reversed-phase column (Alltima™ 4.6 x 250 mm) with a linear gradient
279 of acetonitrile (from 5% to 95%) in 0.05% trifluoroacetic acid solution over 25 min. After
280 identification by mass spectrometry (LCMS-2020, Shimadzu), the peptides were lyophilized for
281 storage.

282

283 4.2. Cryoprotective tests for LDH

284

285 The cryoprotective activities of peptides for LDH were estimated by the inhibition of
286 cryoinactivation and cryodenaturation. The methods were described previously (Hara et al., 2017)
287 with slight modifications.

288 For the cryoinactivation test, 30 μL of each peptide solution (0, 0.033, 0.33, 3.3, 8.3, 17, 33, 83,
289 170, and 500 μM) in 10 mM Tris-HCl buffer pH 7.5 was mixed with 20 μL of LDH solution (0.34
290 μM as a monomer) in 1.5-mL plastic tubes. The tubes were frozen in liquid N_2 for 1 min and then
291 transferred to a water bath at $25\pm 2^\circ\text{C}$ for 3 min to thaw the ice. These freeze-thaw cycles were done
292 three times. The LDH activities of the thawed samples were measured. The LDH reaction was
293 initiated by adding peptide-containing LDH solution (4 μL) to a reaction solution (196 μL , 9.5 mM
294 Tris-HCl pH 7.5, 0.58 mM sodium pyruvate, and 60 μM NADH). The reaction was monitored by
295 measuring absorbance at 340 nm in a microplate reader (Varioskan Flash, Thermo Fisher Scientific,
296 Tokyo, Japan) at 25 $^\circ\text{C}$. Usually, the three freeze-thaw cycles reduced the LDH activity to 15 to 20%
297 of the initial activity. One-hundred-percent cryoinactivation means a decreased degree of LDH
298 activity by the freeze and thaw process. The inhibition activities of peptides for cryoinactivation
299 were evaluated as a 50% protection dose (PD_{50}). In order to calculate PD_{50} , we routinely used the
300 data of relative cryoinactivation at 100 μM for the maximal protection if two requirements were
301 fulfilled: 1) the relative cryoinactivation at 100 μM was less than 20% and 2) the relative
302 cryoinactivation at 100 μM ranged from 50% to 100% of the value at 50 μM . When the relative
303 cryoinactivation was higher than 50% even at 300 μM , PD_{50} was represented as more than 300 μM .

304 The cryodenaturation of LDH was analyzed by using the fluorescence of ANS, which can detect
305 hydrophobic regions on a protein surface. Samples (250 μL) containing ANS (10 μM), LDH (4 μM),
306 and peptides (0, 2, 5, 10, 20, 60, and 100 μM) in 10 mM sodium phosphate buffer pH 7.0 were
307 prepared in 1.5-ml plastic tubes. After the three freeze-thaw cycles as described above, fluorescence
308 at Ex 350 nm/Em 470 nm was determined (Varioskan Flash). The samples with no peptide (0 μM)
309 showed remarkable fluorescence after the three freeze-thaw cycles. The increment of fluorescence in
310 the sample without peptide was 100%. A 50% protection dose (PD_{50}) was used to represent the
311 inhibition of cryodenaturation. When the relative cryodenaturation at 100 μM was less than 20% and
312 the relative cryodenaturation at 100 μM ranged from 50% to 100% of the value at 50 μM , the value
313 at 100 μM was used for the maximal protection. If the relative cryodenaturation was higher than
314 50% even at 60 μM , PD_{50} was represented as more than 60 μM .

315

316 4.3. Circular dichroism (CD)

317

318 Secondary structures of peptides (Fseg and Fseg_Φ/T) were analyzed by CD. Samples containing
319 the peptides (60 μM), SDS (0.1, 1, and 10 mM) and Tris-HCl buffer pH 7.5 (10 mM) were subjected
320 to a spectropolarimeter (J-820, Jasco, Tokyo, Japan). The measurement conditions were as follows:
321 scan range from 195 to 250 nm, scan speed 100 nm min⁻¹, resolution 1 nm, and cell width 2 mm.

322

323 *4.4. Peptide structures*

324

325 Predicted structures of peptides were produced by using the online server PEP-FOLD3
326 (<http://bioserv.rpbs.univ-paris-diderot.fr/services/PEP-FOLD3/>) (Lamiable et al., 2016). The
327 structures were built as in the neutral solution. The most relevant model with the best TM score was
328 chosen. The results are shown in Supplemental Fig. 3.

329

330 *4.5. Statistical analysis*

331

332 Data for *P* values were analyzed by Dunnett's test at a significance level of 0.05.

333

334 **Acknowledgement** This study was supported by a Grant-in-Aid (No. 18H02222) for Scientific
335 Research from the Ministry of Education, Culture, Sports, Science, and Technology of Japan.

336

337 **Declarations of interest** None.

338

339 **References**

340 Ágoston, B.S., Kovács, D., Tompa, P., Perczel, A., 2011. Full backbone assignment and dynamics of
341 the intrinsically disordered dehydrin ERD14. *Biomol. NMR Assign.* 5, 189-193.

342

343 Alsheikh, M.K., Heyen, B.J., Randall, S.K., 2003. Ion binding properties of the dehydrin ERD14 are
344 dependent upon phosphorylation. *J. Biol. Chem.* 278, 40882-40889.

345

346 Banerjee, A., Roychoudhury, A., 2016. Group II late embryogenesis abundant (LEA) proteins:
347 structural and functional aspects in plant abiotic stress. *Plant Growth Regul.* 79, 1-17.

348

349 Boddington, K.F., Graether, S.P., 2019. Binding of a *Vitis riparia* Dehydrin to DNA. *Plant Science*,
350 110172.

351

352 Bravo, L.A., Gallardo, J., Navarrete, A., Olave, N., Martinez, J., Alberdi, M., Close, T.J., Corcuera,

353 L.J., 2003. Cryoprotective activity of a cold-induced dehydrin purified from barley. *Physiol. Plant.*
354 118, 262-269.
355

356 Chakrabortee, S., Tripathi, R., Watson, M., Schierle, G.S., Kurniawan, D.P., Kaminski, C.F., Wise,
357 M.J., Tunnacliffe, A., 2012. Intrinsically disordered proteins as molecular shields. *Mol. Biosyst.* 8,
358 210-219.
359

360 Clarke, M.W., Boddington, K.F., Warnica, J.M., Atkinson, J., McKenna, S., Madge, J., Barker, C.H.,
361 Graether, S.P., 2015. Structural and functional insights into the cryoprotection of membranes by the
362 intrinsically disordered dehydrins. *J. Biol. Chem.* 290, 26900-26913.
363

364 Close, T.J., 1997. Dehydrins: a commonality in the response of plants to dehydration and low
365 temperature. *Physiol. Plant.* 100, 291-296.
366

367 Cuevas-Velazquez, C.L., Reyes, J.L., Covarrubias, A.A., 2017. Group 4 late embryogenesis
368 abundant proteins as a model to study intrinsically disordered proteins in plants. *Plant signal. behav.*
369 12, 10893-10903.
370

371 Davis, J.G., Gierszal, K.P., Wang, P., Ben-Amotz, D., 2012. Water structural transformation at
372 molecular hydrophobic interfaces. *Nature* 491, 582-585.
373

374 Drira, M., Saibi, W., Brini, F., Gargouri, A., Masmoudi, K., Hanin, M., 2013. The K-segments of the
375 wheat dehydrin DHN-5 are essential for the protection of lactate dehydrogenase and β -glucosidase
376 activities in vitro. *Mol. Biotech.* 54, 643-650.
377

378 Eriksson, S.K., Harryson, P., 2011. Dehydrins: Molecular Biology, Structure and Function, in: Lüttge,
379 U., Beck, E., Bartels, D. (Eds.), *Plant Desiccation Tolerance. Ecological Studies (Analysis and*
380 *Synthesis)*, vol 215. Springer, Berlin, Heidelberg, pp. 289-305.
381

382 Eriksson, S.K., Kutzer, M., Procek, J., Gröbner, G., Harryson, P., 2011. Tunable membrane binding
383 of the intrinsically disordered dehydrin Lti30, a cold-induced plant stress protein. *Plant Cell* 23,
384 2391-2404.
385

386 Findlater, E.E., Graether, S.P., 2009. NMR assignments of the intrinsically disordered K 2 and YSK
387 2 dehydrins. *Biomol. NMR Assign.* 3, 273-275.
388

389 Graether, S.P., Boddington, K.F., 2014. Disorder and function: a review of the dehydrin protein
390 family. *Front. Plant Sci.* 5, 576.
391
392 Hand, S.C., Menze, M.A., Toner, M., Boswell, L., Moore, D., 2011. LEA proteins during water
393 stress: not just for plants anymore. *Annu. Rev. Physiol.* 73, 115-134.
394
395 Hanin, M., Brini, F., Ebel, C., Toda, Y., Takeda, S., 2011. Plant dehydrins and stress tolerance:
396 versatile proteins for complex mechanisms. *Plant Signal. Behav.* 6, 1503-1509.
397
398 Hara, M., Endo, T., Kamiya, K., Kameyama, A., 2017. The role of hydrophobic amino acids of
399 K-segments in the cryoprotection of lactate dehydrogenase by dehydrins. *J. Plant Physiol.* 210,
400 18-23.
401
402 Hara, M., Fujinaga, M., Kuboi, T., 2005. Metal binding by citrus dehydrin with histidine-rich
403 domains. *J. Exp. Bot.* 56, 2695-2703.
404
405 Hara, M., Kondo, M., Kato, T., 2013. A KS-type dehydrin and its related domains reduce
406 Cu-promoted radical generation and the histidine residues contribute to the radical-reducing
407 activities. *J. Exp. Bot.* 64, 1615-1624.
408
409 Hara, M., Shinoda, Y., Tanaka, Y., Kuboi, T., 2009. DNA binding of citrus dehydrin promoted by
410 zinc ion. *Plant Cell Environ.* 32, 532-541.
411
412 Hara, M., Terashima, S., Fukaya, T., Kuboi, T., 2003. Enhancement of cold tolerance and inhibition
413 of lipid peroxidation by citrus dehydrin in transgenic tobacco. *Planta* 217, 290-298.
414
415 Hara, M., Terashima, S., Kuboi, T., 2001. Characterization and cryoprotective activity of
416 cold-responsive dehydrin from *Citrus unshiu*. *J. Plant Physiol.* 158, 1333-1339.
417
418 Hernández-Sánchez, I.E., Martynowicz, D.M., Rodríguez-Hernández, A.A., Pérez-Morales, M.B.,
419 Graether, S.P., Jiménez-Bremont, J.F., 2014. A dehydrin-dehydrin interaction: the case of SK3 from
420 *Opuntia streptacantha*. *Front Plant. Sci.* 5, 520.
421
422 Hughes, S., Graether, S.P., 2011. Cryoprotective mechanism of a small intrinsically disordered
423 dehydrin protein. *Protein Sci.* 20, 42-50.
424

425 Hughes, S.L., Schart, V., Malcolmson, J., Hogarth, K.A., Martynowicz, D.M., Tralman-Baker, E.,
426 Patel, S.N., Graether, S.P., 2013. The importance of size and disorder in the cryoprotective effects of
427 dehydrins. *Plant Physiol.* 163, 1376-1386.
428

429 Hundertmark, M., Hinch, D.K., 2008. LEA (late embryogenesis abundant) proteins and their
430 encoding genes in *Arabidopsis thaliana*. *BMC Genom.* 9, 118.
431

432 Koag, M.C., Wilkens, S., Fenton, R.D., Resnik, J., Vo, E., Close, T.J., 2009. The K-segment of maize
433 DHN1 mediates binding to anionic phospholipid vesicles and concomitant structural changes. *Plant*
434 *Physiol.* 150, 1503-1514.
435

436 Lamiable, A., Thévenet, P., Rey, J., Vavrusa, M., Derreumaux, P., Tufféry, P., 2016. PEP-FOLD3:
437 faster de novo structure prediction for linear peptides in solution and in complex. *Nucl. Acid. Res.* 44,
438 W449-W454.
439

440 Liu, X., Zhang, C.S., Lu, C., Lin, S.C., Wu, J.W., Wang, Z.X., 2016. A conserved motif in
441 JNK/p38-specific MAPK phosphatases as a determinant for JNK1 recognition and inactivation.
442 *Nature Commun.* 7, 10879.
443

444 Mace, P.D., Wallez, Y., Egger, M.F., Dobaczewska, M.K., Robinson, H., Pasquale, E.B., Riedl, S.J.,
445 2013. Structure of ERK2 bound to PEA-15 reveals a mechanism for rapid release of activated
446 MAPK. *Nature Commun.* 4, 1681.
447

448 Nylander, M., Svensson, J., Palva, E.T., Welin, B., 2001. Stress-induced accumulation and tissue
449 specific localization of dehydrins in *Arabidopsis thaliana*. *Plant Mol. Biol.* 45, 263-279.
450

451 Ochoa-Alfaro, A.E., Rodríguez-Kessler, M., Pérez-Morales, M.B., Delgado-Sánchez, P.,
452 Cuevas-Velazquez, C.L., Gómez-Anduro, G., Jiménez-Bremont, J.F., 2012. Functional
453 characterization of an acidic SK 3 dehydrin isolated from an *Opuntia streptacantha* cDNA library.
454 *Planta* 235, 565-578.
455

456 Palmer, S.R., De Villa, R., Graether, S.P., 2019. Sequence composition versus sequence order in the
457 cryoprotective function of an intrinsically disordered stress-response protein. *Protein Sci.* 28,
458 1448-1459.
459

460 Peng, Y., Reyes, J.L., Wei, H., Yang, Y., Karlson, D., Covarrubias, A.A., Krebs, S.L., Fessehaie, A.,

461 Arora, R., 2008. RcDhn5, a cold acclimation-responsive dehydrin from *Rhododendron catawbiense*
462 rescues enzyme activity from dehydration effects in vitro and enhances freezing tolerance in
463 RcDhn5 - overexpressing *Arabidopsis* plants. *Physiol. Plant.* 134, 583-597.
464

465 Puhakainen, T., Hess, M.W., Mäkelä, P., Svensson, J., Heino, P., Palva, E.T., 2004. Overexpression
466 of multiple dehydrin genes enhances tolerance to freezing stress in *Arabidopsis*. *Plant Mol. Biol.* 54,
467 743-753.
468

469 Rahman, L.N., Smith, G.S., Bamm, V.V., Voyer-Grant, J.A., Moffatt, B.A., Dutcher, J.R., Harauz, G.,
470 2011. Phosphorylation of *Theellungiella salsuginea* dehydrins TsDHN-1 and TsDHN-2 facilitates
471 cation-induced conformational changes and actin assembly. *Biochemistry* 50, 9587-9604.
472

473 Reyes, J.L., Campos, F., Wei, H.U.I., Arora, R., Yang, Y., Karlson, D.T., Covarrubias, A.A., 2008.
474 Functional dissection of hydrophilins during in vitro freeze protection. *Plant Cell Environ.* 31,
475 1781-1790.
476

477 Strimbeck, G.R., 2017. Hiding in plain sight: the F segment and other conserved features of seed
478 plant SKn dehydrins. *Planta* 245, 1061-1066.
479

480 Tompa, P., Csermely, P., 2004. The role of structural disorder in the function of RNA and protein
481 chaperones. *FASEB J.* 18, 1169-1175.
482

483 Wei, H., Yang, Y., Himmel, M.E., Tucker, M.P., Ding, S.Y., Yang, S., Arora, R., 2019. Identification
484 and characterization of five cold stress-related rhododendron dehydrin genes: spotlight on a
485 FSK-type dehydrin with multiple F-segments. *Front. Bioeng. Biotech.* 7, 30.
486

487 Xing, X., Liu, Y., Kong, X., Liu, Y., Li, D., 2011. Overexpression of a maize dehydrin gene,
488 ZmDHN2b, in tobacco enhances tolerance to low temperature. *Plant Growth Regul.* 65, 109-118.
489

490 Yang, W., Zhang, L., Lv, H., Li, H., Zhang, Y., Xu, Y., Yu, J., 2015. The K-segments of wheat
491 dehydrin WZY2 are essential for its protective functions under temperature stress. *Front Plant Sci*
492 6:406.
493

494 Zhang, A., Qi, W., Singh, S.K., Fernandez, E.J., 2011. A new approach to explore the impact of
495 freeze-thaw cycling on protein structure: hydrogen/deuterium exchange mass spectrometry
496 (HX-MS). *Pharm. Res.* 28, 1179-1193.

497

498 Zhang, H., Shi, Y., Liu, X., Wang, R., Li, J., Xu, J., 2018. Transgenic creeping bentgrass plants
499 expressing a *Picea wilsonii* dehydrin gene (PicW) demonstrate improved freezing tolerance. Mol.
500 Biol. Rep. 45, 1627-1635.

501

502 **Figure legends**

503

504 **Fig. 1.** Cryoprotective activities of typical K-segment (TypK) and *Arabidopsis* F-segments. (A)
505 Peptide names, corresponding dehydrins, and amino acid sequences are shown. Inhibition of
506 cryoinactivation (B) and that of cryodenaturation (C) of lactate dehydrogenase (LDH) by the
507 peptides are shown as PD₅₀. Values shown are the means of three experiments. Columns and bars
508 represent means ± SD. No significant difference ($p < 0.05$) from TypK.

509

510 **Fig. 2.** Cryoprotective activities of Fseg and its related peptides (amino acid substitutions). (A)
511 Amino acid sequences of the peptides. Fseg means COR47Fseg in Fig. 1. Φ, +, and - represent
512 hydrophobic, positively charged, and negatively charged amino acids, respectively. Letters of
513 hydrophobic amino acids are shaded. Inhibition of cryoinactivation (B) and that of cryodenaturation
514 (C) were evaluated as PD₅₀. Values shown are the means of three experiments. Columns and bars
515 represent means ± SD. Asterisks indicate significant differences ($p < 0.05$) from Fseg. When the
516 PD₅₀ values were more than 300 μM in B and 60 μM in C, the tops of the columns were shredded. In
517 these cases, asterisks are not labeled.

518

519 **Fig. 3.** Cryoprotective activities of Fseg and its related peptides (G substitutions). (A) Amino acid
520 sequences of the peptides. Fseg means COR47Fseg in Fig. 1. Φ, +, and - represent hydrophobic,
521 positively charged, and negatively charged amino acids, respectively. Letters of hydrophobic amino
522 acids are shaded. Inhibition of cryoinactivation (B) and that of cryodenaturation (C) were evaluated
523 as PD₅₀. Values shown are the means of three experiments. Columns and bars represent means ± SD.
524 Asterisks indicate significant differences ($p < 0.05$) from Fseg. When the PD₅₀ values were more
525 than 300 μM in B and 60 μM in C, the tops of the columns are shredded. In these cases, asterisks are
526 not labeled.

527

528 **Fig. 4.** Analyses of secondary structures of Fseg and Fseg_Φ/T. (A) Circular dichroism analysis for

529 Fseg and Fseg_Φ/T. Effects of sodium dodecyl sulfate (SDS) on their secondary structures are
530 shown. Gray broken lines, gray solid lines, black broken lines, and black solid lines represent 0, 0.1,
531 1, and 10 mM SDS, respectively. (B) Predictive quantification of the secondary structure
532 compositions in Fseg and Fseg_Φ/T by using K2D2
533 (<http://cbdm-01.zdv.uni-mainz.de/~andrade/k2d2/>). The CD data in A were used. Black, gray, and
534 white columns show α-helix, β-strand, and others (random structures), respectively. Values shown
535 are the means of three experiments. Bars represent SD. An asterisk indicates a significant difference
536 ($p < 0.05$) from the control sample (0 mM SDS).

537

538 **Fig. 5.** Putative mechanisms for cryoprotective activity of Fseg. When target proteins (e.g., LDH)
539 are frozen and thawed, hydrophobic patches appear on the surface of the proteins, and then
540 hydrophobic interaction is generated between the patches (A). Fseg intervenes in the hydrophobic
541 interaction via its hydrophobic area. While Fseg inhibits hydrophobic binding, hydrophobic
542 hydration may cover the patches. Finally, the native state of proteins was maintained (B). Besides
543 that, Fseg_Φ/T cannot intervene in the hydrophobic interaction because it does not have a
544 hydrophobic area. A water-tight seal forms between the hydrophobic patches of the target proteins
545 after exclusion of Fseg_Φ/T. As a result, the proteins are aggregated (C).

546

547 **Supplemental Figure legends**

548

549 **Supplemental Fig. 1.** *Arabidopsis* FSKn dehydrins. (A) Amino acid sequences of four *Arabidopsis*
550 FSKn dehydrins. F-segments are highlighted in green. Red letters indicate K-segments. (B)
551 Information on the four FSKn dehydrins. Cold-responsive expressions were determined according to
552 the data from the *Arabidopsis* eFP Browser (<http://bar.utoronto.ca/efp/cgi-bin/efpWeb.cgi>).

553

554 **Supplemental Fig. 2.** Cryoprotective tests for lactate dehydrogenase (LDH). (A) Scheme of the
555 assay. Samples containing LDH, peptides, and buffer were treated with three freeze and thaw cycles,
556 after which enzyme activities and denaturation levels were determined. For peptides, Fseg
557 (COR47Fseg) and Fseg_Φ/T (COR47Fseg_Φ/T) were used. (B) Relative cryoinactivation of LDH
558 (%). Values and bars represent means ± SD (three experiments). (C) Relative cryodenaturation of
559 LDH (%). The denaturation levels were monitored by fluorescence (ex 350 nm, em 470 nm) from

560 8-anilino-1-naphthalene sulfonic acid (ANS). Values and bars represent means \pm SD (three
561 experiments).

562

563 **Supplemental Fig. 3A, B.** Predicted peptide structures of F-segments. The structures were built
564 using PEP-FOLD3 (<http://bioserv.rpbs.univ-paris-diderot.fr/services/PEP-FOLD3/>). Structures of
565 Fseg (A) and Fseg_Φ/T (B) are shown. Hydrophobic areas are indicated by yellow elliptical
566 shadows. N and C refer to the N- and C-termini, respectively. Single-letter codes with numbers are
567 positions of amino acid residues in the peptides.

568

569 **Supplemental Fig. 3C.** Predicted peptide structures of F-segments. The structures were built by
570 PEP-FOLD3 (<http://bioserv.rpbs.univ-paris-diderot.fr/services/PEP-FOLD3/>). Structures of
571 ERD10Fseg, ERD14Fseg, At4g38410Fseg, pG_Fseg_Φ, and TypK are shown. Hydrophobic areas
572 are indicated by yellow elliptical shadows. N and C refer to the N- and C-termini, respectively.
573 Single-letter codes with numbers are positions of amino acid residues in the peptides.

574

575 **Supplemental Fig. 4.** An alignment of amino acid sequences of *Arabidopsis* COR47 and the
576 orthologues from other plant species. All five dehydrins are classified as FSK3 types. *Arabidopsis*,
577 *Rhododendron*, *Malus*, *Nicotiana*, and *Theobroma* represent COR47 from *Arabidopsis*, dehydrin 2
578 (AGI36547) from *Rhododendron catawbiense*, dehydrin COR47-like (NP_001315732) from *Malus*
579 *domestica*, dehydrin (BAD13499) from *Nicotiana tabacum*, and dehydrin 2 (EOY15190) from
580 *Theobroma cacao*, respectively. Asterisks are identical amino acids between species. Black, gray,
581 and white columns represent F-, S-, and K-segments, respectively.

582

583

584

585

586

587

588

589

590

591

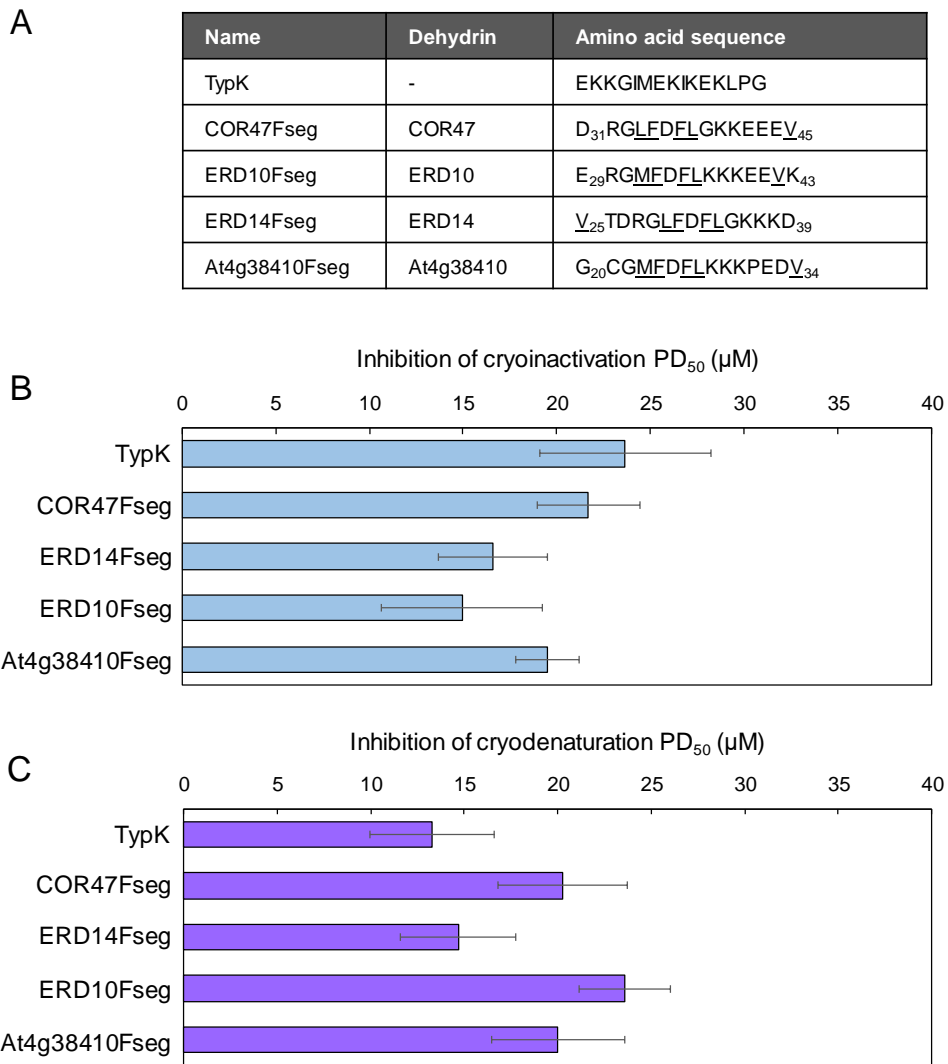


Fig. 1 Ohkubo et al.

592

593

A

	1	2	3	4	5	6	7	8	9	1	1	1	1	1	1
	-	+		Φ	Φ	-	Φ	Φ		0	1	2	3	4	5
										+	+	-	-	-	Φ
Fseg	D	R	G	L	F	D	F	L	G	K	K	E	E	E	V
Fseg_Φ/T	D	R	G	T	T	D	T	T	G	K	K	E	E	E	T
Fseg_DE/T	T	R	G	L	F	T	F	L	G	K	K	T	T	T	V
Fseg_KR/T	D	T	G	L	F	D	F	L	G	T	T	E	E	E	V
Fseg_Φ/E	D	R	G	E	E	D	E	E	G	K	K	E	E	E	E
Fseg_Φ/K	D	R	G	K	K	D	K	K	G	K	K	E	E	E	K

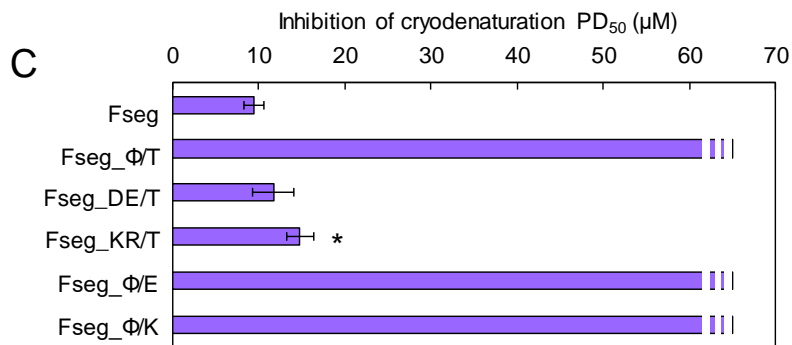
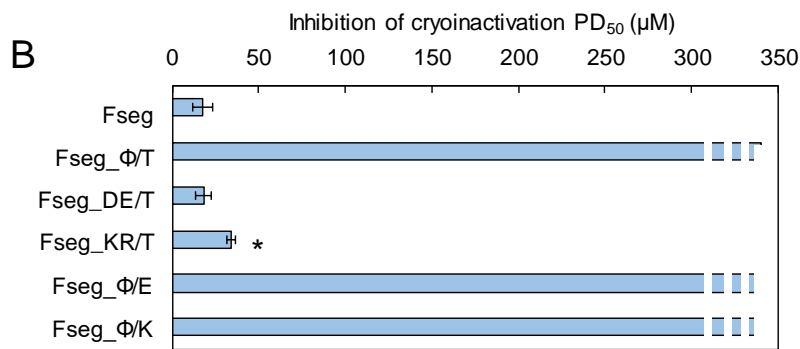


Fig. 2 Ohkubo et al.

594
595

A

	1	2	3	4	5	6	7	8	9	1	1	1	1	1	1
	-	+		Φ	Φ	-	Φ	Φ		0	1	2	3	4	5
	+									+	+	-	-	-	Φ
Fseg	D	R	G	L	F	D	F	L	G	K	K	E	E	E	V
pG_Fseg_Φ	G	G	G	L	F	G	F	L	G	G	G	G	G	G	V
pG_Fseg_ΦDE	D	G	G	L	F	D	F	L	G	G	G	E	E	E	V
pG_Fseg_ΦKR	G	R	G	L	F	G	F	L	G	K	K	G	G	G	V
pG_Fseg_DE	D	G	G	G	G	D	G	G	G	G	G	E	E	E	G
pG_Fseg_KR	G	R	G	G	G	G	G	G	G	K	K	G	G	G	G
pG_Fseg_DEKR	D	R	G	G	G	D	G	G	G	K	K	E	E	E	G

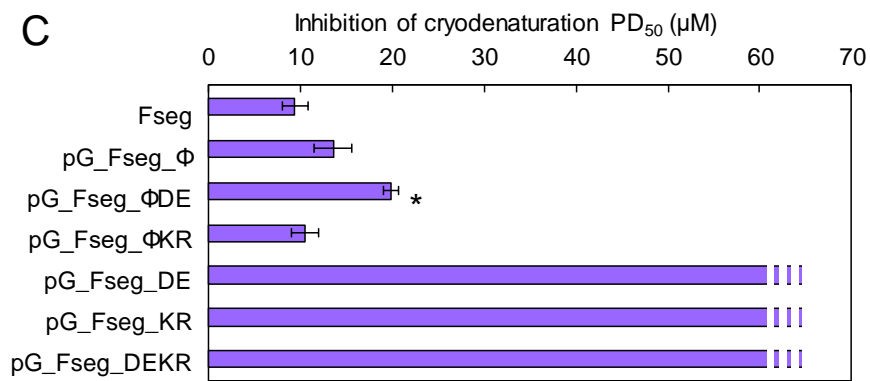
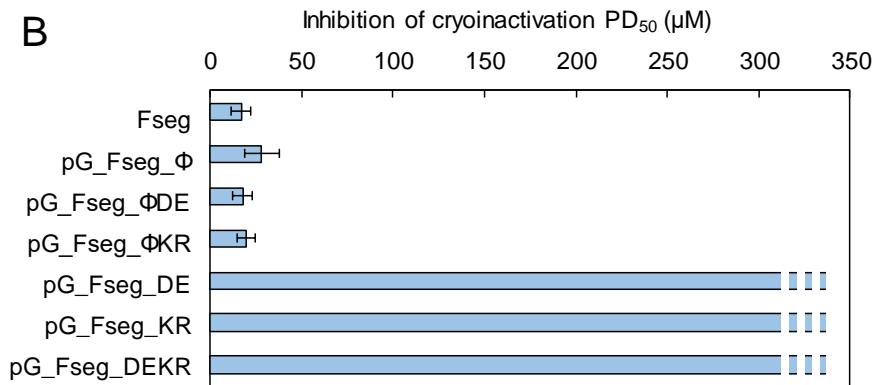


Fig. 3 Ohkubo et al.

596

597

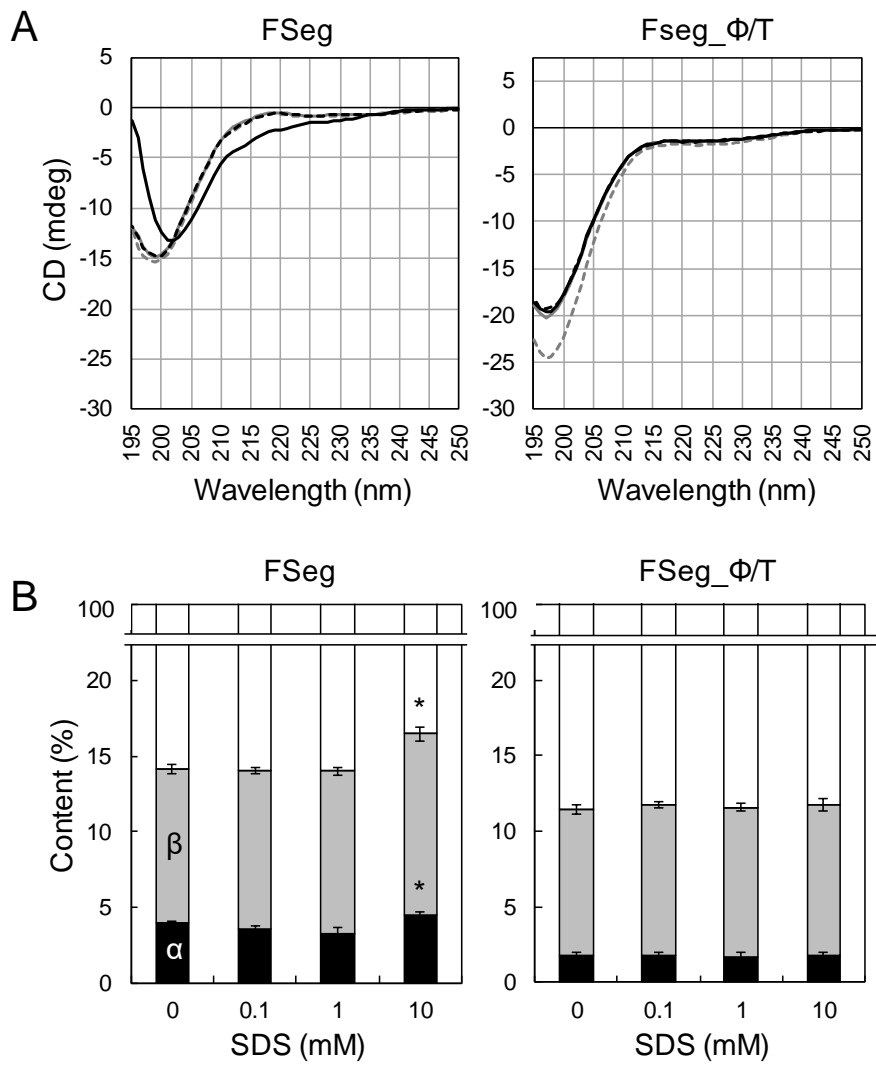


Fig. 4 Ohkubo et al.

598

599

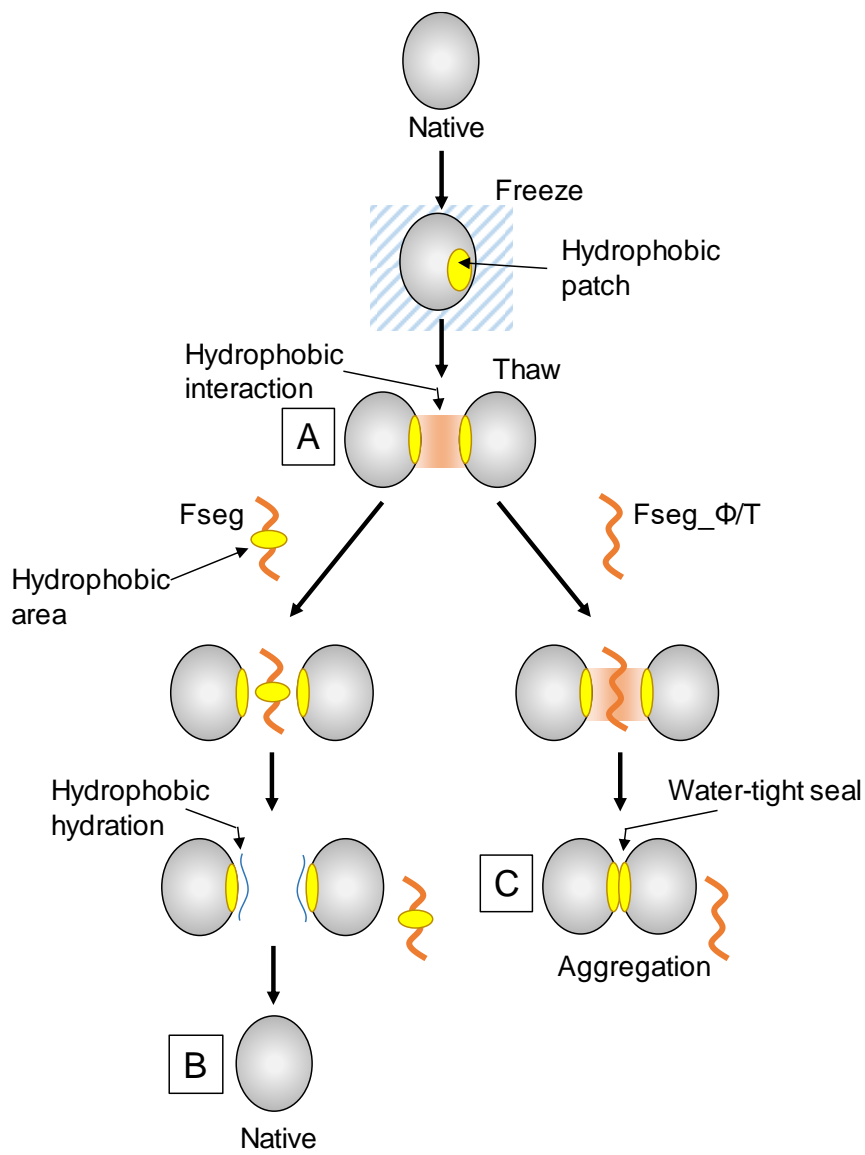


Fig. 5 Ohkubo et al.

600

601

A

◆At1g20440 COR47 (FSK3)
MAEEYKNNVPEHETPTVATEESPATTT EVT **DRGLDFDLGKKKEEV**KPQETTTLESEFDHKAQISEPEL
AAEHVEEVKENKITLLEELQEKT EEEENKPSVIEKLHRSN SSSSSSSSDEEGEEKKEKKKKIVEGEE **DKKG**
LVEKIKEKLPGHHDKTAEDDVPVSTTIPVPVSES VVEHDHPEE **EKKGLVEKIKEKLP**GHHDKAEDSPA
VTSTPLVVTEHPVEPTTELPVEHPE **EKKGILEKIKEKLP**GYHAKTTEEEVKKEKESDD

◆At1g20450 ERD10 (FSK3)
MAEEYKNTVPEQETPKVATEESSAPEIK **ERGMFDLKKKKEEV**KPQETTTLASEFEHKTQISEPESFVAK
HEEEHKTPTLLEQLHQKHEEEENKPSLLDKLHRSN SSSSSSSSDEEGEDGEKKKKEKKKKIVEGDHVK
TVEEE **NQGVMDRIKFKPL**GKPGGDDVPVVTMPAPHSVEDHKPEEE **EKKGFMDKIKEKLP**GHHSK
PEDSQVVNTTPLVETATPIADIPE **EKKGFMDKIKEKLP**GYHAKTTGEEKKKEKVSDD

◆At1g76180 ERD14 (FSK2)
MAEEIKNVPEQEVKPVATEESSAEV **TDRLDFDLGKKK**DKETKPEETPIASEFEQKVHISEPEPEVKHESL
LEKLHRS DSSSSSSSEEGSDGEKRKKKKEKKKPTTEVEVKEE **EKKGFMEKIKDKLP**GHKKPEDGSA
VAAAPVVVPPPVEEAHPV **EKKGILEKIKEKLP**GYHPKTTVEEEKKDKKE

◆At4g38410 (FSK2)
MADHPRSTEQQEADAAASK **GCGMFDLKKKPEDV**HSSSENARVTKEPK EEEKPSLAERFHLSDSSSSD
EEAGENGKKEKKEKKEKNEVAEDQCETEEKIPAGIGHEDG **KEKGFMEKIKDKLP**GGHNGKPEAEPH
NDKAK **KEKGFMEKIKEKLP**GHTNDEKKKET

B

Dehydrin	Gene ID	Dehydrin type	Size (amino acids)	Expression
COR47	At1g20440	FSK3	265	Cold
ERD10	At1g20450	FSK3	260	Cold
ERD14	At1g76180	FSK2	185	Cold
At4g38410	At4g38410	FSK2	163	Cold

Supplemental Fig. 1. *Arabidopsis* FSKn dehydrins. (A) Amino acid sequences of four *Arabidopsis* FSKn dehydrins. F-segments are highlighted in green. Red letters indicate K-segments. (B) Information on the four FSKn dehydrins. Cold-responsive expressions were determined according to the data from the *Arabidopsis* eFP Browser (<http://bar.utoronto.ca/efp/cgi-bin/efpWeb.cgi>).

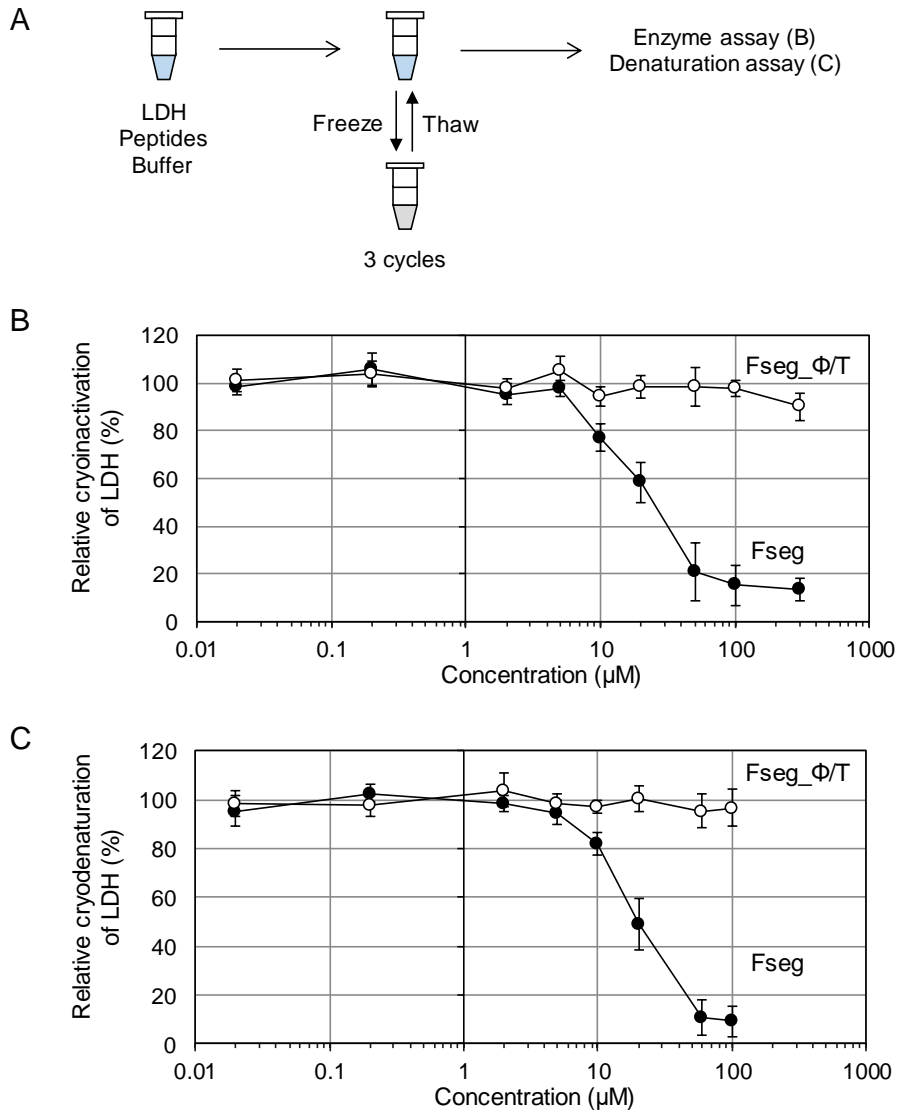
Title: F-segments of *Arabidopsis* dehydrins show cryoprotective activities for lactate dehydrogenase depending on the hydrophobic residues.

Authors: Ohkubo T, Kameyama A, Kamiya K, Kondo M, Hara M*

*hara.masakazu@shizuoka.ac.jp

602

603



Supplemental Fig. 2. Cryoprotective tests for lactate dehydrogenase (LDH). (A) Scheme of the assay. Samples containing LDH, peptides, and buffer were treated with three freeze and thaw cycles, after which enzyme activities and denaturation levels were determined. For peptides, Fseg (COR47Fseg) and Fseg_Φ/T (COR47Fseg_Φ/T) were used. (B) Relative cryoinactivation of LDH (%). Values and bars represent means \pm SD (three experiments). (C) Relative cryodenaturation of LDH (%). The denaturation levels were monitored by fluorescence (ex 350 nm, em 470 nm) from 8-anilino-1-naphthalene sulfonic acid (ANS). Values and bars represent means \pm SD (three experiments).

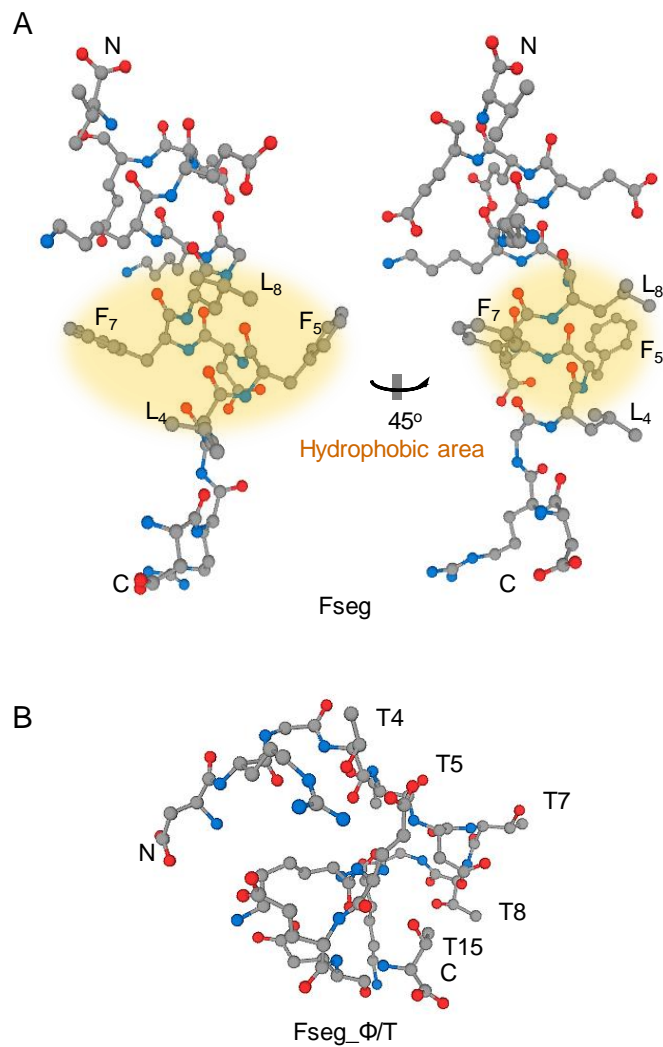
Title: F-segments of *Arabidopsis* dehydrins show cryoprotective activities for lactate dehydrogenase depending on the hydrophobic residues.

Authors: Ohkubo T, Kameyama A, Kamiya K, Kondo M, Hara M*

*hara.masakazu@shizuoka.ac.jp

604

605



Supplemental Fig. 3A, B. Predicted peptide structures of F-segments. The structures were built using PEP-FOLD3 (<http://bioserv.rpbs.univ-paris-diderot.fr/services/PEP-FOLD3/>). Structures of Fseg (A) and Fseg_Φ/T (B) are shown. Hydrophobic areas are indicated by yellow elliptical shadows. N and C refer to the N- and C-termini, respectively. Single-letter codes with numbers are positions of amino acid residues in the peptides.

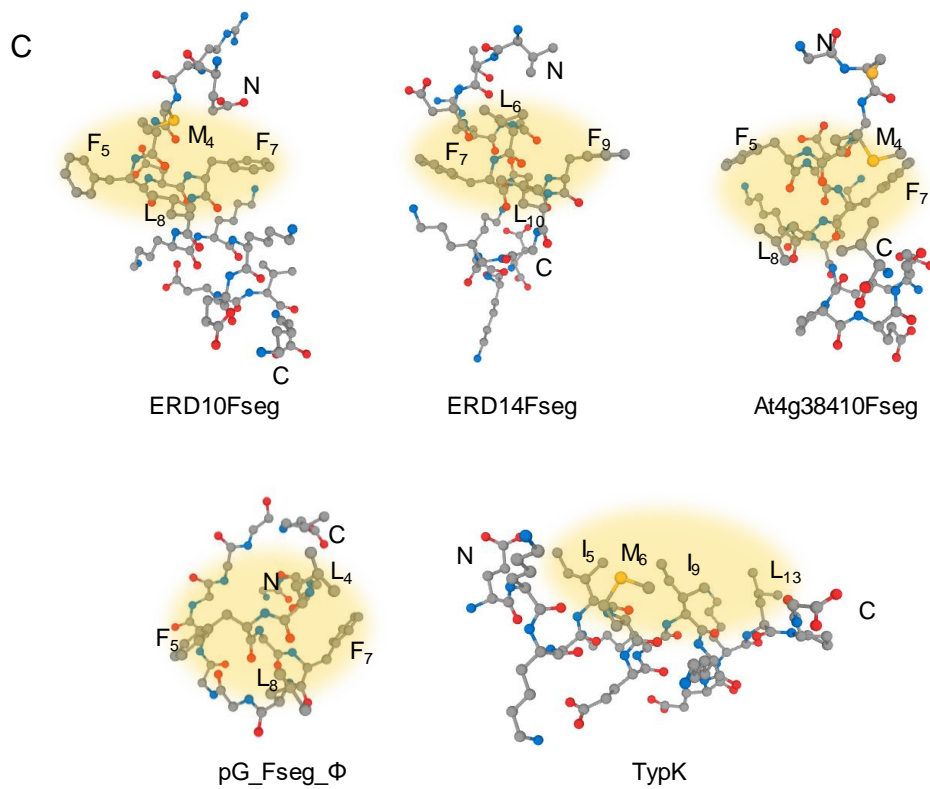
Title: F-segments of *Arabidopsis* dehydrins show cryoprotective activities for lactate dehydrogenase depending on the hydrophobic residues.

Authors: Ohkubo T, Kameyama A, Kamiya K, Kondo M, Hara M*

*hara.masakazu@shizuoka.ac.jp

606

607



Supplemental Fig. 3C. Predicted peptide structures of F-segments. The structures were built by PEP-FOLD3 (<http://bioserv.rpbs.univ-paris-diderot.fr/services/PEP-FOLD3/>). Structures of ERD10Fseg, ERD14Fseg, At4g38410Fseg, pG_Fseg_Φ, and TypK are shown. Hydrophobic areas are indicated by yellow elliptical shadows. N and C refer to the N- and C-termini, respectively. Single-letter codes with numbers are positions of amino acid residues in the peptides.

Title: F-segments of *Arabidopsis* dehydrins show cryoprotective activities for lactate dehydrogenase depending on the hydrophobic residues.

Authors: Ohkubo T, Kameyama A, Kamiya K, Kondo M, Hara M*

*hara.masakazu@shizuoka.ac.jp

608

609

